



# Influence of single photon emission computed tomography (SPECT) reconstruction algorithm on diagnostic accuracy of parathyroid scintigraphy: Comparison of iterative reconstruction with filtered backprojection

Gonca Kara Gedik & Oktay Sari

*Department of Nuclear Medicine, School of Medicine, Selcuk University, Konya, Turkey*

Received February 25, 2015

**Background & objectives:** Preoperative localization of parathyroid lesions is essential for improving the results in patients with primary hyperparathyroidism. The purpose of this study was to evaluate retrospectively the value of technetium-99m (Tc-99m) methoxyisobutylisonitrile (MIBI) single photon emission computed tomography (SPECT) and to compare the diagnostic accuracy of iterative reconstruction (IR) and filtered backprojection (FBP) reconstruction algorithms about localization of parathyroid lesions.

**Methods:** Forty four patients with primary hyperparathyroidism, in whom histopathological correlation could be performed, were included in the study. Dual-phase Tc-99m parathyroid scintigraphy was performed 20 and 120 min after injection of 740 MBq Tc-99m MIBI in all patients. Tomographic images were acquired 120 min after the administration of radiopharmaceutical. The SPECT data were evaluated using an IR as well as a FBP algorithm. In 23 of 44 patients, SPECT acquisitions were performed in 64×64 matrix; in the remaining 21 patients, tomographic data were collected in 128×128 matrix. The imaging results were compared with pathological findings and sensitivities of both reconstruction algorithms, and planar views were calculated.

**Results:** Using planar MIBI scans, abnormal parathyroid glands were correctly localized in 75 per cent of the cases. Sensitivity increased to 77 per cent using SPECT with FBP and to 84 per cent with IR. When the sensitivities were calculated according to the acquisition matrix, these were 95 per cent (20/21) and 85 per cent (18/21) for IR and FBP, respectively in patients in whom 128×128 matrix was used. The sensitivities were lower in patients who were imaged with 64×64 matrix; these were calculated as 74 per cent (17/23) and 70 per cent (16/23) with IR and FBP, respectively.

**Interpretation & conclusions:** Our findings showed that compared to planar scintigraphy, Tc-99m MIBI SPECT was more sensitive diagnostic modality in the detection of abnormal parathyroid tissues. Image quality and sensitivity may be improved further when larger matrices with IR are used instead of FBP algorithm.

**Key words** Hyperparathyroidism - reconstruction - single photon emission computed tomography - technetium-99m methoxyisobutylisonitrile

Primary hyperparathyroidism is a common endocrine disorder of calcium, phosphate and bone metabolism caused by excess secretion of parathormone (PTH). The majority of cases of primary hyperparathyroidism (85%) are caused by single hyperfunctioning adenoma<sup>1</sup>. Parathyroid hyperplasia accounts for <15 per cent of cases and parathyroid carcinoma represents <1 per cent of cases of primary hyperparathyroidism<sup>1</sup>.

Considering that a solitary adenoma is the most frequent cause of primary hyperparathyroidism, the surgery of primary hyperparathyroidism has moved on from the traditional bilateral neck exploration, which consists of extensive bilateral dissection, identifying all four glands and removing the enlarged ones, to limited surgical approaches such as image-guided unilateral parathyroidectomy. The success of this type of surgery, however, depends on the accurate preoperative localization of the parathyroid lesion, and several anatomical and functional preoperative localizing techniques for abnormal parathyroid tissue have been developed<sup>1</sup>. Currently technetium-99m (Tc-99m) methoxyisobutylisonitrile (MIBI) parathyroid scintigraphy is the preferred imaging protocol in the preoperative localization of parathyroid lesions<sup>2</sup>. For MIBI scintigraphy, both dual-phase technique and the double-tracer subtraction technique have been proved to be sensitive in detecting of parathyroid adenomas<sup>3</sup>. Moreover, single photon emission computed tomography (SPECT), which provides advantage about improvement of contrast enhancement, can also be added to standard planar MIBI scintigraphy. Further, use of radiopharmaceuticals, instrumentation, data acquisition, image reconstruction and processing techniques allowed the use of SPECT in clinical practice<sup>4</sup>.

For SPECT evaluation, the data may be reconstructed using the methods of iterative reconstruction (IR) or filtered backprojection (FBP) in parathyroid scintigraphy<sup>1,5</sup>. FBP may produce streak artefacts, but it is widely used in clinical SPECT because of its simplicity, speed and computational efficiency. IR algorithms promise noise suppression, reducing artefacts and improved resolution. This retrospective study was aimed to compare the diagnostic accuracy of two different reconstruction algorithms for detection of parathyroid lesions using parathyroid SPECT with Tc-99m MIBI.

### Material & Methods

The medical records of 90 patients, who underwent dual-phase Tc-99m MIBI parathyroid scintigraphy at

School of Medicine, Selcuk University, Konya, Turkey, between March 2011 and September 2014, were retrospectively evaluated. Only those patients were selected who were surgically and histopathologically correlated and with PTH levels returned to normal values after surgery. Therefore, 44 patients who were not operated and one patient in whom persistent hyperparathyroidism was observed after surgical procedure were excluded. One patient with chronic renal failure and with tertiary hyperparathyroidism was also excluded from the study. Finally, 44 patients with primary hyperparathyroidism (37 women and 7 men, age range: 26-76 yr, mean age 53.75±12.39 yr), with mean serum PTH and calcium levels of 241.97±210.7 (range: 65-940 pg/ml and reference value: 12-65 pg/ml) and 11.30±0.88 mg/dl (range: 10-14.4 mg/dl and reference value: 8.4-10.2 mg/dl), respectively, were included in the study. The study was approved by the local Ethics Committee of Selcuk University, Faculty of Medicine (No: 2012-223).

The preoperative localization imaging workup included dual-phase Tc-99m MIBI planar parathyroid scintigraphy and SPECT. Planar images were obtained 20 (early phase) and 120 min (delayed phase) after intravenous administration of 740 MBq (20 mCi) Tc-99m MIBI (MON-MIBI KIT, Eczacıbası-Monrol, Turkey) on a dual headed gamma camera (Siemens, Ecam-signature, Germany) equipped with a low-energy, a high-resolution parallel-hole collimator. Anterior and posterior planar views centred on the cervical and thoracic areas were acquired in supine position using 256×256 matrix, a time acquisition of five minutes per view. SPECT imaging of neck and upper chest was performed 120 min after injection of Tc-99m MIBI. SPECT acquisition obtained 64 views over 360° at 30 sec per view with elliptical orbit. In 23 patients, 64×64 matrix was used, pixel size was 9.6 mm; in the remaining 21 patients, 128×128 matrix and 4.8 mm pixel size were the adopted parameters of the SPECT acquisition. In all patients, images were reconstructed using two different algorithms: FBP and IR. For FBP, a low-pass post processing filter with a cut-off frequency of 0.85 cycles/cm was used. SPECT data were reconstructed with ordered subsets expectation maximization (OS-EM), 16 subsets and four iterations in IR. The transverse, frontal and sagittal slices and also the planar images were visually analyzed independently by two experienced nuclear medicine physicians who were blinded to the results of histopathology. A focus of increased activity in the

neck or mediastinum that persisted on delayed imaging in contrast to the decreased activity in thyroid was considered as parathyroid pathology for late planar imaging. A nodular formation or irregularity of the posterior side of the thyroid gland was interpreted as a parathyroid lesion on reconstructed SPECT slices. Considering the histopathology as the gold standard, late planar scintigraphy and SPECT imaging were classified as true positive (TP), true negative (TN), false negative (FN) and false positive (FP). Parathyroid adenomas, hyperplastic parathyroid tissues and carcinomatous parathyroid glands were considered as TP findings. Normal parathyroid glands were classified as TN. A parathyroid lesion missed by imaging procedures was considered as FN and accumulation of radiotracer in a non-parathyroid lesion was considered as FP. Sensitivity was calculated on a per-lesion basis.

### Results

Bilateral neck exploration was performed in all patients. Elevated serum calcium and PTH levels returned to normal values after surgery in all patients. Forty four parathyroid lesions were resected from the same number of patients.

Of the 44 parathyroid lesions, 40 (91%) were parathyroid adenomas, three (7%) were hyperplastic parathyroid tissues and one lesion (2%) was reported as parathyroid carcinoma. Delayed planar scintigraphy detected 70 per cent (31/44) of parathyroid lesions. In two patients, parathyroid lesions were visualized only on early images (Fig. 1). Combined early and delayed planar imaging detected 75 per cent (33/44) of all parathyroid lesions. SPECT imaging increased the sensitivity of parathyroid scintigraphy to 84 per cent (37/44) with IR algorithm. The sensitivity of SPECT with FBP was calculated as 77 per cent (34/44). When the sensitivity was further calculated according to the acquisition matrix, it was found that in patients in whom 128×128 matrix was used, the sensitivity was 95 (20/21) and 85 per cent (18/21) for IR and FBP, respectively. On the other hand, sensitivity was lower in patients who were imaged with 64×64 matrix; with IR, it was calculated as 74 per cent (17/23) whereas, with FBP, the sensitivity was 70 per cent (16/23). The demographics of patients, the results of pathology and reconstruction algorithms according to the acquisition matrix are shown in Table I.

SPECT imaging with FBP missed 10 lesions which were pathologically proved as abnormal glands (adenoma in 7 patients, carcinoma in 1 and hyperplasia

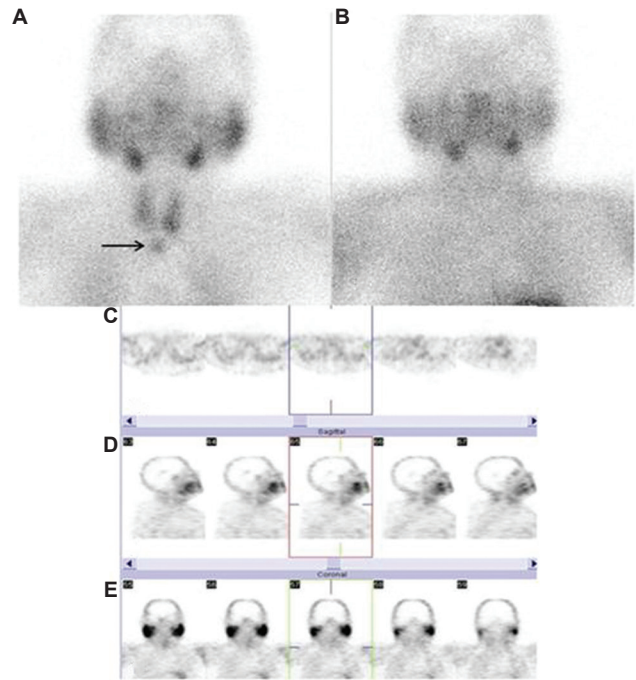


**Fig. 1.** Early (A) and late (B) planar views of dual-phase technetium 99m methoxyisobutylisonitrile parathyroid scintigraphy. A parathyroid lesion, which later confirmed as parathyroid adenoma, showed rapid radiopharmaceutical washout. Early planar view showed the lesion (A, arrow). Transaxial (C), sagittal (D) and coronal (E) slices of single photon emission computed tomography study (with 64×64 matrix) which was reconstructed with iterative reconstruction algorithm. The focus was detectable neither on late planar view nor on single photon emission computed tomography study with both reconstruction algorithms (patient no: 42, Table I).

in 2 patients), whereas IR algorithm produced seven FN results (adenoma in 5 patients, carcinoma in 1 and hyperplasia in 1 patient). Three patients, who were reported as FN with FBP, could be interpreted as TP with IR (Figs. 2 and 3). Among the patients reported false-negative, in whom IR was used, SPECT acquisition was performed with 128×128 matrix in one patient, and in the remaining six, 64×64 matrix was used. For the 10 patients who were reported as FN with FBP, 128×128 matrix was used in three and 64×64 in the remaining seven. The effect of acquisition matrix on image quality was obvious when FBP, instead of IR was used (Fig. 4). In two patients in whom early but not late planar scintigraphy depicted abnormal parathyroid lesions, SPECT study was acquired in 64×64 matrix, and the results of SPECT were negative with both reconstruction algorithms. The distribution of TP and FN results according to reconstruction algorithm and acquisition matrix is shown in Table II.

In one patient (patient no: 37, Table I), Tc-99m accumulation was observed in lower poles of right

**Table I.** Demographics of patients and results of laboratory, scintigraphy and pathology

Patient number	Age (yr)	Gender	PTH level (pg/ml)	Calcium level (mg/dl)	Late planar view	SPECT acquisition matrix	SPECT with IR	SPECT with FBP	Pathology
1	64	Female	171	11.1	+, TP	64×64	+, TP	+, TP	Hyperplasia
2	53	Male	842	12.4	+, TP	128×128	+, TP	+, TP	Adenoma
3	43	Female	292	10.8	+, TP	128×128	+, TP	+, TP	Adenoma
4	60	Male	157	13.1	+, TP	128×128	+, TP	+, TP	Adenoma
5	72	Female	280	10.4	+, TP	64×64	+, TP	+, TP	Adenoma
6	53	Female	94.33	10.9	-, FN	64×64	-, FN	-, FN	Adenoma
7	47	Female	65	10.9	+, TP	128×128	+, TP	+, TP	Adenoma
8	31	Female	122	11.7	+, TP	128×128	+, TP	+, TP	Adenoma
9	42	Female	456	11.0	+, TP	128×128	+, TP	+, TP	Adenoma
10	26	Female	189	11.2	-, FN	128×128	+, TP	+, TP	Adenoma
11	50	Male	97.97	10.6	+, TP	128×128	+, TP	+, TP	Adenoma
12	74	Male	199	12.6	+, TP	128×128	+, TP	+, TP	Adenoma
13	52	Female	141	11.3	+, TP	128×128	+, TP	+, TP	Adenoma
14	43	Female	183.3	10.7	+, TP	128×128	+, TP	+, TP	Adenoma
15	51	Female	199.8	12.2	+, TP	128×128	+, TP	+, TP	Adenoma
16	72	Female	124	10.3	+, TP	128×128	+, TP	-, FN	Adenoma
17	65	Female	117.5	11.7	+, TP	128×128	+, TP	+, TP	Adenoma
18	64	Female	88.64	10.2	-, FN	128×128	+, TP	-, FN	Adenoma
19	63	Female	81.7	11.4	+, TP	64×64	+, TP	+, TP	Adenoma
20	69	Female	320	11.1	+, TP	64×64	+, TP	+, TP	Adenoma
21	62	Female	166	12.0	+, TP	64×64	+, TP	+, TP	Adenoma
22	69	Female	111	10.2	+, TP	64×64	+, TP	+, TP	Adenoma
23	47	Female	238	10.7	+, TP	64×64	+, TP	+, TP	Adenoma
24	43	Female	202	11.0	-, FN	64×64	-, FN	-, FN	Carcinoma
25	31	Female	494	11.67	+, TP	64×64	+, TP	+, TP	Adenoma
26	44	Female	214	11.2	+, TP	64×64	+, TP	+, TP	adenoma
27	76	Female	111	10.6	+, TP	64×64	+, TP	-, FN	Hyperplasia
28	47	Female	173	14.4	+, TP	64×64	+, TP	+, TP	Adenoma
29	36	Female	300	10.6	-, FN	64×64	+, TP	+, TP	Adenoma
30	49	Male	70.09	10	+, TP	64×64	+, TP	+, TP	Adenoma
31	66	Female	849.3	12.4	-, FN	64×64	+, TP	+, TP	Adenoma
32	76	Male	654.9	12.5	+, TP	64×64	+, TP	+, TP	Adenoma
33	46	Female	262.1	11.4	+, TP	64×64	+, TP	+, TP	Adenoma
34	49	Female	940	11.7	+, TP	128×128	+, TP	+, TP	Adenoma
35	49	Female	112	11.9	+, TP	128×128	+, TP	+, TP	Adenoma
36	49	Male	349	12.5	+, TP	128×128	+, TP	+, TP	Adenoma
37	50	Female	107	10.8	-, FN	128×128	+, TP	+, TP	Adenoma
38	54	Female	86	11.01	-, FN	128×128	-, FN	-, FN	Hyperplasia
39	54	Female	161.8	11.07	-, FN	64×64	-, FN	-, FN	Adenoma
40	64	Female	153.3	10.8	-, FN	64×64	-, FN	-, FN	Adenoma

*Contd...*

Patient number	Age (yr)	Gender	PTH level (pg/ml)	Calcium level (mg/dl)	Late planar view	SPECT acquisition matrix	SPECT with IR	SPECT with FBP	Pathology
41	40	Female	83.63	10.2	-, FN	128×128	+, TP	+, TP	Adenoma
42	59	Female	228	10.8	-, FN	64×64	-, FN	-, FN	Adenoma
43	60	Female	225.4	11.5	-, FN	64×64	-, FN	-, FN	Adenoma
44	51	Female	134	10.7	+, TP	64×64	+, TP	+, TP	Adenoma

+, reported as positive; -, reported as negative; TP, true positive; FN, false negative; IR, iterative reconstruction; FBP, filtered backprojection; SPECT, single photon emission computed tomography; PTH, parathormone

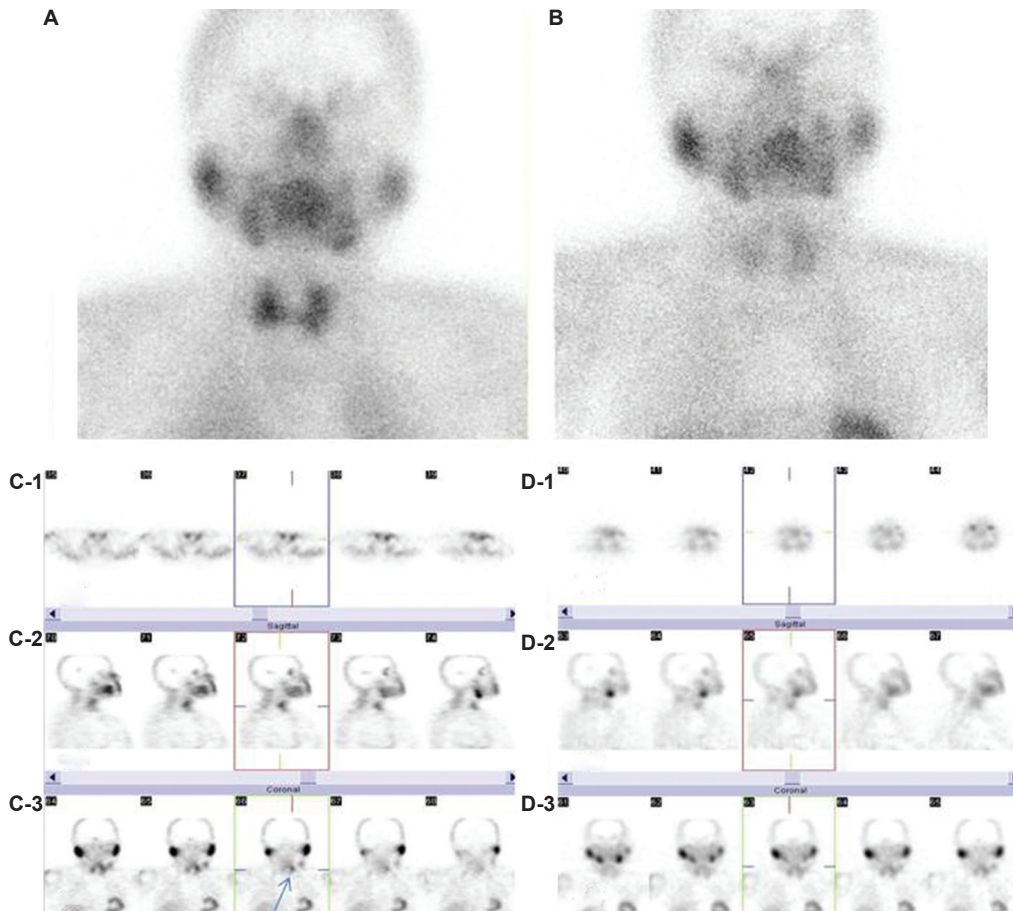


**Fig. 2.** Early (A) and late (B) planar views of technetium-99m methoxyisobutylisonitrile parathyroid scintigraphy. Transaxial (C-1), sagittal (C-2) and coronal (C-3) slices of technetium-99m methoxyisobutylisonitrile single-photon emission computed tomography study which was acquired in 128×128 matrix were generated using iterative reconstruction algorithm. Parathyroid pathology was depicted in the upper pole of left thyroid lobe (C-3, arrow). However, the focus was not detectable on images analyzed with filtered backprojection algorithm, transaxial (D-1), sagittal (D-2) and coronal (D-3) views (patient no: 18, Table 1).

and left thyroid lobes with both reconstruction algorithms. Histopathological investigation revealed parathyroid adenoma and Hashimoto’s thyroiditis in thyroid gland.

Tc-99m MIBI accumulation was not observed in normal parathyroid glands neither on planar views nor on SPECT studies.

### Discussion

Parathyroid scintigraphy is used to preoperatively localize the parathyroid lesion causing primary hyperparathyroidism. Since Tc-99m MIBI was introduced as a parathyroid imaging agent in 1989, excellent results for localization of parathyroid adenomas have been reported by many investigators

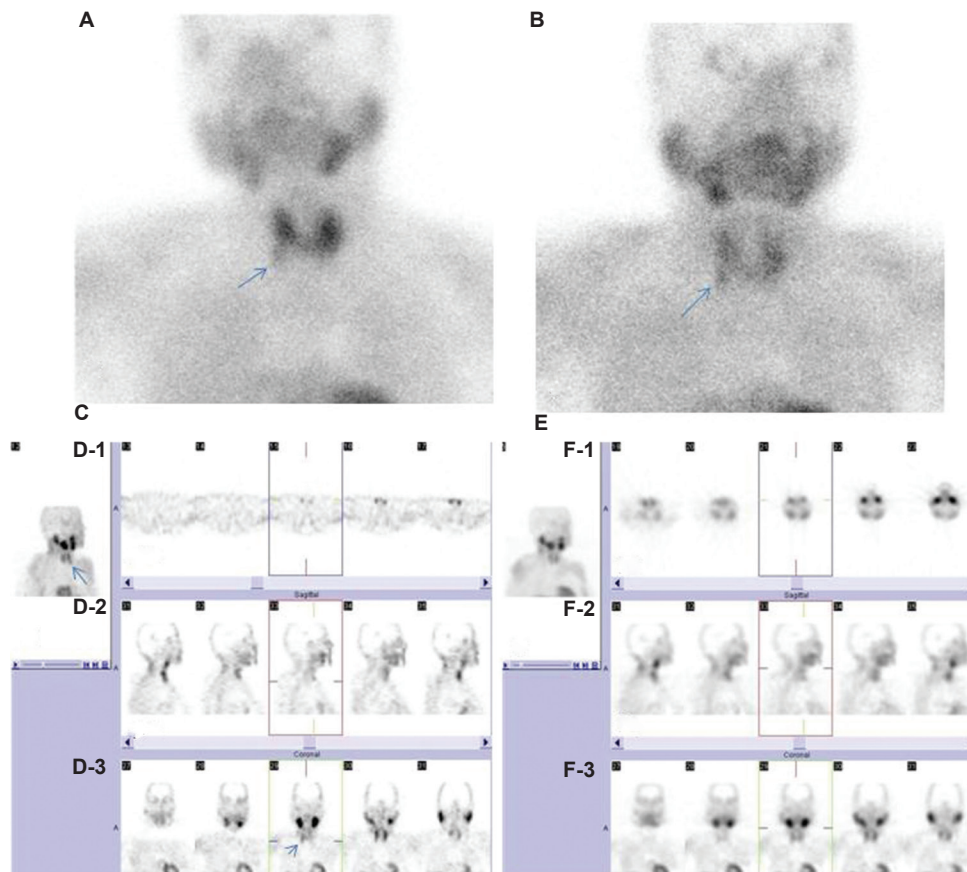


**Fig. 3.** A focus of increased activity was observed on early (A) and late (B) planar views (A-B, arrows). Three-dimensional image of single photon emission computed tomography study with iterative reconstruction (C-arrow), clearly depicted parathyroid lesion. Transaxial (D-1), sagittal (D-2) and coronal (D-3) slices of technetium-99m methoxyisobutylisonitrile single photon emission computed tomography study, faintly demonstrated the radioactivity retention in the lower part of right thyroid lobe (D-3, arrow). Delineation of hyperplastic parathyroid tissue could not be possible either on three-dimensional (E) or on transaxial (F-1), sagittal (F-2) and coronal (F-3) views of single photon emission computed tomography study with filtered backprojection, (patient no: 27, Table I).

**Table II.** Distribution of true-positive and false-negative results according to the reconstruction algorithm and acquisition matrix

Acquisition matrix	Results	IR	FBP	Total number of patients
128	TP	20	18	21
	FN	1	3	
64	TP	17	16	23
	FN	6	7	

TP, true positive; FN, false negative; IR, iterative reconstruction; FBP, filtered backprojection

using different imaging protocols<sup>6</sup>. SPECT is a useful component of planar imaging and can be added to dual-phase parathyroid scintigraphy. It has been shown that SPECT offers increased sensitivity and provides more accurate information about the localization of abnormal parathyroid glands<sup>7-9</sup>. However, some

parathyroid lesions do not retain MIBI and some extraparathyroidal lesions can accumulate and retain MIBI leading to both false-negative and false-positive results.

High sensitivity of SPECT is desirable for accurate detection of parathyroid lesion. Both biologic factors such as gland size and type, mitochondrial/subcellular structure and p-glycoprotein expression and technical factor such as spatial resolution influence the sensitivity of SPECT for the detection of pathological parathyroid tissue<sup>8</sup>. The sensitivity of SPECT may vary from 78 to 96 per cent<sup>9</sup>. This variability may be secondary to difference of acquisition protocols between studies, functional and histopathological characteristics of the glands. In our study, the sensitivity of SPECT was 84 per cent which was higher than the sensitivity of planar imaging (75%). Moka *et al*<sup>10</sup> reported a sensitivity of 95 per cent with SPECT compared

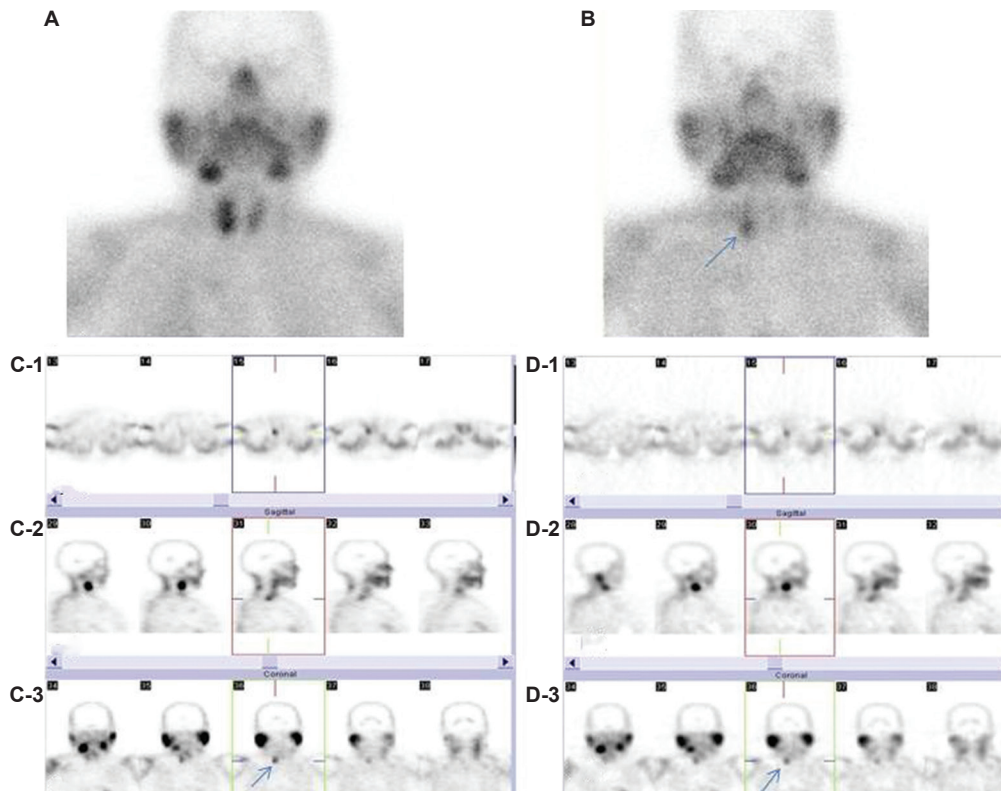


**Fig. 4.** Early (A) and late (B) planar views. Single photon emission computed tomography study was performed using with  $64 \times 64$  matrix. Transaxial (C-1), sagittal (C-2) and coronal (C-3) slices of technetium-99m methoxyisobutylisonitrite single photon emission computed tomography study which were reconstructed using with iterative reconstruction. A parathyroid lesion was delineated in the lower pole of right thyroid lobe (C-3, arrow). The same parathyroid lesion could also be depicted in the lower pole of right thyroid lobe with filtered backprojection algorithm (D-3, arrow). However, streak artefacts were present on transaxial slices (D-1), and image degradation was observed compared to iterative reconstruction algorithm (patient no: 22, Table I).

to a sensitivity of 87 per cent for planar imaging. Lorberboym *et al*<sup>3</sup> showed that SPECT increased the sensitivity from 79 to 96 per cent. In our study, in two patients, parathyroid lesions were detected only with early planar imaging, late planar and SPECT studies with both reconstruction algorithms revealed negative results (patient numbers: 24 and 42, Table I). This is a limitation of the dual-phase technique; parathyroid adenomas with rapid washout may cause FN results on late imaging. The number of oxyphil cells in parathyroid lesions is reported to have an effect on this phenomenon and a small number of oxyphil cells may account for rapid washout of Tc-99m MIBI<sup>3</sup>. To avoid this, acquiring of SPECT study following early planar acquisition is generally recommended<sup>1</sup>.

The SPECT method requires projection images to be acquired from different angles around the patient. These planar images are reconstructed using image reconstruction methods which generate cross-section images of the internally distributed

radiopharmaceuticals. Since FBP has been the only reconstruction algorithm available on almost all commercial computer platforms and because of its simple implementation, FBP has been widely used in SPECT reconstruction for many years. FBP has now been replaced by IR which has a potential to correct a wide range of image degrading effects. However, FBP can still be used as a reconstruction algorithm for processing the SPECT data, and its applicability to the parathyroid SPECT dataset has been reported<sup>1</sup>.

The effect of the type of reconstruction software on the image quality of SPECT data has been shown<sup>11,12</sup>. The influence of two commercially available IR algorithms on the image quality and diagnostic accuracy of SPECT has been studied. Image quality has been shown to be affected by SPECT reconstruction algorithm and its influence is higher than the performance of the gamma camera. Moka *et al*<sup>10</sup> assessed the value of Tc-99m MIBI SPECT and IR algorithm for the preoperative localization of parathyroid adenomas and found that

sensitivity and image quality were improved when IR was used instead of FBP. The effect of reconstruction algorithm on image quality was obvious in our study also; the sensitivity increased from 77 to 84 per cent, when IR instead of FBP was used. The sensitivity of IR was calculated higher than FBP in both acquisition matrices. However, sensitivities of both algorithms were found to be lower than the results by Moka *et al*<sup>10</sup>, where all SPECT acquisitions were performed with 128×128 matrix. In our study, in patients who were imaged with 128×128 matrix, the sensitivity of SPECT study was 95 and 85 per cent with IR and FBP, respectively. We reached a similar sensitivity as that of Moka *et al*<sup>10</sup> (95 vs. 97%) with IR in patients who were imaged with 128×128 matrix; however, the sensitivity of SPECT with FBP was still lower (85 vs. 94%). Marked decrease in the sensitivity of SPECT data was observed in patients who were imaged with 64×64 matrix (74% and 70% with IR and FBP, respectively).

The matrix size used in acquiring the projection data of SPECT plays an important role in the quality of the reconstructed image because it determines the degree of spatial details that can be presented. To improve the resolution of acquired data, choosing the maximum possible matrix size is desirable; the visual quality of images improves as the pixel size decreases. Hence, higher SPECT resolution will be achieved with the smaller pixel size of 128×128 matrix than with a pixel size of 64×64 (in our study, 4.8 vs. 9.6 mm, respectively). When large matrices are used for small areas, statistical fluctuation increases. This low signal-to-noise ratio can be reduced by smoothing, but spatial resolution will decrease. For parathyroid SPECT studies, 128×128 matrix resolution acquisition is usually recommended<sup>1,5</sup>; however, in practice, 64×64 acquisitions may also be used<sup>2,4,13</sup>. The quality of tomographic image generated from FBP depends on the number of acquired projections. Streak artefacts may appear in the reconstructed image if low angular views are obtained. These artefacts cause decrease in image quality, loss of contrast and resolution in the reconstructed image.

The size of abnormal parathyroid gland is another factor that influences the scintigraphic localization of abnormal parathyroid gland. Relatively poor results in the localization of hyperplastic parathyroid glands have been given by scanning techniques<sup>14</sup>. In the only patient who was reported as FN in 128 matrix group with IR algorithm, pathology report was consistent

with parathyroid hyperplasia. Although sizes of the pathologic parathyroid tissues could not be analyzed in our study, perhaps the small size of this hyperplastic tissue played a role.

The most frequent cause of false-positive results in Tc-99m MIBI parathyroid imaging is nodular thyroid lesion either on solitary or in a multinodular gland. Thyroid carcinoma, lymphoma, lymphadenopathy and inflammation are other causes of false-positive results of MIBI accumulation<sup>15</sup>. In our study, false positivity was observed only in one patient, in whom, Hashimoto's thyroiditis was reported histopathologically apart from the parathyroid lesion. Although the cellular uptake of Tc-99m MIBI uptake is mainly attributable to membrane electron potentials and passive diffusion, transporters are known to play important roles in its cellular efflux and excretion<sup>9,14</sup>. The presence of significant p-glycoprotein expression prevents accumulation of Tc-99m MIBI<sup>14</sup>. It has been demonstrated that during inflammation, the expression of various transporters is altered in rodents<sup>16</sup>. In the brain, expression of p-glycoprotein has been shown to be downregulated by locally induced inflammation<sup>16</sup>. This mechanism may explain the observation of Tc-99m MIBI accumulation in Hashimoto's thyroiditis in our study.

The limitation of our study was its retrospective design. Besides, size and weight analysis of pathological parathyroid glands could not be performed.

In conclusion, our results showed that SPECT was more sensitive for detection of abnormal parathyroid glands than planar MIBI scans. IR algorithm with larger matrices improved the resolution of the reconstructed image and increased the sensitivity compared to FBP.

**Conflicts of Interest:** None.

## References

- Hindié E, Ugur O, Fuster D, O'Doherty M, Grassetto G, Ureña P, *et al* 2009 EANM parathyroid guidelines. *Eur J Nucl Med Mol Imaging* 2009; 36 : 1201-16.
- Rubello D, Casara D, Pagetta C, Piotta A, Pelizzo MR, Shapiro B. Determinant role of Tc-99m MIBI SPECT in the localization of a retrotracheal parathyroid adenoma successfully treated by radioguided surgery. *Clin Nucl Med* 2002; 27 : 711-5.
- Lorberboym M, Minski I, Macadzio S, Nikolov G, Schachter P. Incremental diagnostic value of preoperative <sup>99m</sup>Tc-MIBI SPECT in patients with a parathyroid adenoma. *J Nucl Med* 2003; 44 : 904-8.
- Billotey C, Sarfati E, Aurengo A, Duet M, Mündler O, Toubert ME, *et al*. Advantages of SPECT in technetium-99m-

- sestamibi parathyroid scintigraphy. *J Nucl Med* 1996; 37 : 1773-8.
5. Greenspan BS, Dillehay G, Intenzo C, Lavelly WC, O'Doherty M, Palestro CJ, *et al.* SNM practice guideline for parathyroid scintigraphy 4.0. *J Nucl Med Technol* 2012; 40 : 111-8.
  6. Kettle AG, O'Doherty MJ. Parathyroid imaging: How good is it and how should it be done? *Semin Nucl Med* 2006; 36 : 206-11.
  7. Moka D, Voth E, Dietlein M, Larena-Avellaneda A, Schicha H. Technetium 99m-MIBI-SPECT: A highly sensitive diagnostic tool for localization of parathyroid adenomas. *Surgery* 2000; 128 : 29-35.
  8. Schurrer ME, Seabold JE, Gurll NJ, Simonson TM. Sestamibi SPECT scintigraphy for detection of postoperative hyperfunctional parathyroid glands. *AJR Am J Roentgenol* 1996; 166 : 1471-4.
  9. Ansguer C, Mirallié E, Carlier T, Abbey-Huguenin H, Aubron F, Kraeber-Bodéré F. Preoperative localization of parathyroid lesions. *Nuklearmedizin* 2008; 47 : 158-62.
  10. Moka D, Eschner W, Voth E, Dietlein M, Larena-Avellaneda A, Schicha H. Iterative reconstruction: An improvement of technetium-99m MIBI SPET for the detection of parathyroid adenomas? *Eur J Nucl Med* 2000; 27 : 485-9.
  11. Knoll P, Kotalova D, Köchle G, Kuzelka I, Minear G, Mirzaei S, *et al.* Comparison of advanced iterative reconstruction methods for SPECT/CT. *Z Med Phys* 2012; 22 : 58-69.
  12. van Hoorn RA, Vriens D, Postema JW, Arens AI, Pfestroff A, Oyen WJ, *et al.* The influence of SPECT reconstruction algorithms on image quality and diagnostic accuracy in phantom measurements and <sup>99m</sup>Tc-sestamibi parathyroid scintigraphy. *Nucl Med Commun* 2014; 35 : 64-72.
  13. Rubello D, Piotta A, Casara D, Muzzio PC, Shapiro B, Pelizzo MR. Role of gamma probes in performing minimally invasive parathyroidectomy in patients with primary hyperparathyroidism: Optimization of preoperative and intraoperative procedures. *Eur J Endocrinol* 2003; 149 : 7-15.
  14. Pons F, Torregrosa JV, Fuster D. Biological factors influencing parathyroid localization. *Nucl Med Commun* 2003; 24 : 121-4.
  15. Palestro CJ, Tomas MB, Tronco GG. Radionuclide imaging of the parathyroid glands. *Semin Nucl Med* 2005; 35 : 266-76.
  16. Wang JH, Scollard DA, Teng S, Reilly RM, Piquette-Miller M. Detection of P-glycoprotein activity in endotoxemic rats by <sup>99m</sup>Tc-sestamibi imaging. *J Nucl Med* 2005; 46 : 1537-45.

*Reprint requests:* Dr Gonca Kara Gedik, Department of Nuclear Medicine, School of Medicine, Selcuk University, Konya, Turkey  
e-mail: goncakara@yahoo.com